Measurement of turbulent flow in a square duct with roughened walls on two opposite sides

Hajime Yokosawa
College of General Education, Nagoya University, Nagoya, Japan

Hideomi Fujita, Masafumi Hirota
Department of Mechanical Engineering, Nagoya University, Nagoya, Japan

Shotaro Iwata
Mitsubishi Electric Co. Ltd.

A fully developed turbulent flow along a square duct, two opposite walls of which had been roughened by square cross-sectioned ribs, was measured with a hot-wire anemometer. This paper presents the resulting velocities and stresses and compares them with measurements taken in a square duct with four smooth walls. Symmetrical results, with respect to the axes of symmetry of the duct cross section, were obtained in every measured quantity. Terms on both sides of the vorticity transport equation were calculated, and the balance of terms was discussed. As is well known, smooth-walled square ducts yield two secondary flow cells in any given quadrant of a cross section. But in ducts whose opposite walls have been roughened, we found a hitherto unobserved phenomenon: only one relatively large cell appeared in each quadrant of a duct's cross section.

Keywords: flow measurement; turbulent flow; square duct; roughened wall; secondary flow

Introduction

Noncircular ducts are used often in industry. It is well known that secondary flows of Prandtl's second kind occur in turbulent flows along these ducts. The character of the surface of the walls which makes up a duct strongly influence fluid flows along the ducts. Consequently, it would be more difficult to predict the characteristics of the flow and of the heat transfer in noncircular ducts with rough surfaces. For ducts utilized to transport heat, rough surfaces are used to augment heat transfer. From this point of view, the flows in ducts with rough walls also have attracted interest.[1] Experimental and analytical studies have been reported on flows in straight square ducts, since the form of the cross section is very simple. But most of these studies are of flows in ducts with smooth walls.[2–5] Launder and Ying measured the mean velocity field in a square duct with four rough walls,[6] Humphrey and Whitelaw measured velocity fields and turbulent stress fields in a duct with a rough wall,[7] and Fujita conducted experiments on flows in various square ducts consisting of smooth and rough planes.[8]

According to Fujita's results, there are remarkable differences in distributions of axial flow velocities due to the combination of rough and smooth walls. This suggests that there should also be differences in the secondary flows and in the turbulent stresses which give rise to the secondary flows. Hence, we have conducted accurate measurements of turbulent flows in a square duct with one rough wall[9] and in a rectangular duct with one rough wall.[10]

Address all reprint requests to Professor Yokosawa, College of General Education, Nagoya University, Furocho, Chikusaku, Nagoya 464, Japan.

Received 15 October 1987; accepted for publication 12 December 1988

In this paper, we take a fully developed turbulent flow in a square duct with roughened walls on two opposite sides as an objective of our experiment. The experimental results of the velocity field and turbulent stress field are presented and compared with the results of a duct with four smooth walls.

Experiment

The flow apparatus of this experiment is essentially the same as that used elsewhere for measurements of duct flows similar to the one treated here. An airflow, obtained by a turboblower driven by a variable-speed electric motor, is introduced into a duct after the flow rate is measured by a quadrant flow nozzle. The test duct, whose cross section was 50 mm^2 and 4500 mm long, was made of transparent acrylic resin board with a smooth surface. Roughness elements whose cross section was 1 mm^2 were used to make up the two roughened facing walls of the duct. The elements were placed at 10-mm intervals transverse to the primary flow, as shown in Figure 1, to maximize the resistance to the flow through the duct.[11] Hereafter this duct is referred to as the rough duct. The flow in a smooth duct which is composed on four smooth walls was also measured under the same condition as those of the rough duct so as to provide a comparison with the rough duct.

Static pressures were measured at 250-mm intervals in the axial direction: measurements were conducted in the rough duct by means of a static pressure tube of 1 mm o.d. with a measuring hole of diameter 0.3 mm at the center of the duct; in the smooth duct measurements were conducted by means of static pressure holes 0.3 mm in diameter drilled through an upper wall and a side wall. Local wall shear stresses were measured by a Preston tube 1 mm in o.d. and 0.8 mm in i.d. and calculated from Patel's formula.[12]

Flow measurements were conducted with constant Reynolds number ($\mathrm{Re}=Ud_h/\nu$) 6.5×10^4, where U is bulk mean axial velocity, d_h is hydraulic diameter, and ν is kinematic viscosity of air. Mean and fluctuation velocities were measured at the cross section 5 mm downstream of the roughness element farthest downstream by means of a hot-wire anemometer with an I-wire or an X-wire probe whose sensing part was 1 mm long. In the measurements of stresses and secondary flows, two X-wire probes, mirror images of each other, were used to eliminate errors due to velocity gradient.[13] In order to investigate the effects of roughness elements on the secondary flow pattern, we performed additional measurements at the duct cross section running atop the roughness element farthest downstream.

Figure 1 shows the orthogonal coordinate system, having X_1 axis along the duct and X_2 and X_3 axes parallel to the walls of the duct. Subscripts 1, 2, and 3 denote that the quantities are the components in the direction of the X_1, X_2, and X_3 axes, respectively. Roughness elements are placed on the upper and lower surfaces which are perpendicular to the X_3 axis.

Experimental results and discussion

Coefficient of resistance and wall shear stress

The dimensionless coefficients of resistance to the flows through the ducts were calculated using measured values by the formula:

$$\lambda=\frac{d_h(-\mathrm{d}P/\mathrm{d}X_1)}{\frac{1}{2}\rho U^2} \tag{1}$$

where P is static pressure and ρ is density of the air. The results are shown in Figure 2. In the range of the present experiment ($5\times10^4<\mathrm{Re}<10^5$), values of λ for the rough duct showed the almost constant value $\lambda=0.06$, independent of Reynolds numbers. The magnitude of this value is three times larger than that of the smooth duct. The measured distribution is almost the same as the results noted for a duct with two rough walls roughened by wires of 1 mm in diameter.[8]

Figure 3 shows the distributions of local wall shear stresses on each smooth wall. $\bar{\tau}_w$ denotes the mean value of τ_w on the wall concerned. The Preston tube method is based on the assumption that the velocity distribution is expressed by the wall law. Therefore, the velocity profile in the wall region of the smooth wall was confirmed beforehand to be expressed as

$$U_1/u_\tau=5.5\log(u_\tau y/\nu)+5.4 \tag{2}$$

(in all the region excluding both corners within 5 mm from the side wall), where u_τ denotes the friction velocity, and y is the distance from the wall. The distribution profiles of wall shear stresses are, as Figure 3 clearly shows, similarly independent of Reynolds numbers. Compared to a gentle slope of the profile for the smooth duct, in the rough duct values of $\tau_w/\bar{\tau}_w$ measured on the smooth wall decrease rapidly on approaching the corner of the duct. The mean shear stress for the walls of a duct, $\bar{\tau}$, can be calculated by Equation 1

$$\bar{\tau}=\tfrac{1}{8}\lambda\rho U^2 \tag{3}$$

For the rough duct, there is the following relation between $\bar{\tau}_r$ and $\bar{\tau}_s$, which denotes a mean shear stress for the rough wall

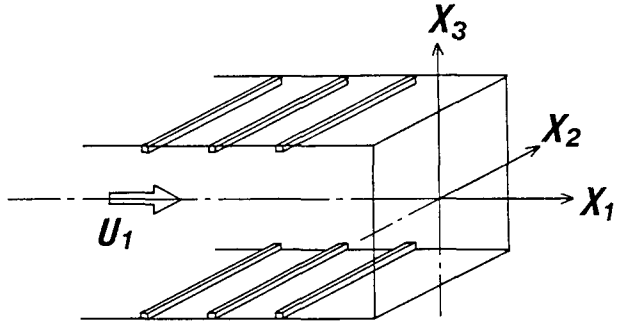

Figure 1 Coordinate system

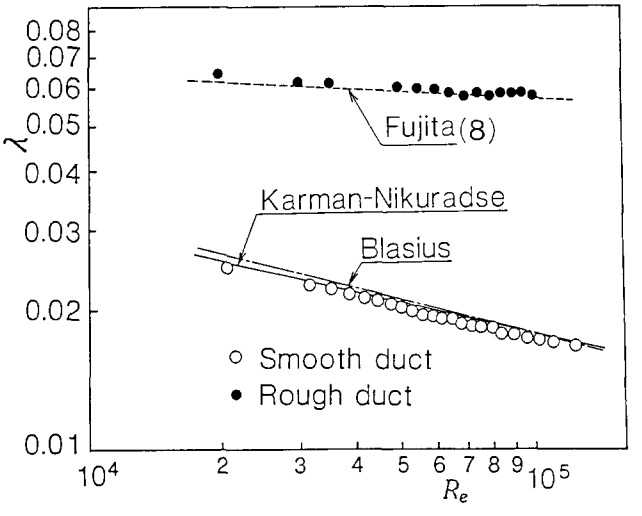

Figure 2 Dimensionless coefficient of resistance to the flow through ducts

Notation

$B=D/2$	Half length of a side
d_h	Hydraulic diameter of duct
D	Length of a side of square duct
h	Turbulent kinetic energy
P	Static pressure
$\mathrm{Re}=Ud_h/\nu$	Reynolds number
$\overline{u_1u_2}$, $\overline{u_1u_3}$	Turbulent shear stresses in X_2 and X_3 directions, respectively
u_τ	Friction velocity
$\sqrt{\overline{u_1^2}}$, $\sqrt{\overline{u_2^2}}$, $\sqrt{\overline{u_3^2}}$	Root mean square of velocity fluctuations in each direction
U	Bulk mean velocity
U_1	Mean velocity in X_1 direction
U_S	U_1 at the center of duct
X_1, X_2, X_3	Orthogonal coordinates
y	Distance from wall
λ	Coefficient of resistance
ν	Kinematic viscosity of fluid
ρ	Density of fluid
$\bar{\tau}$	Mean wall shear stress
τ_w	Local wall shear stress
Ω_1	Vorticity in X_1 direction
Subscripts	
r	Rough wall
s	Smooth wall

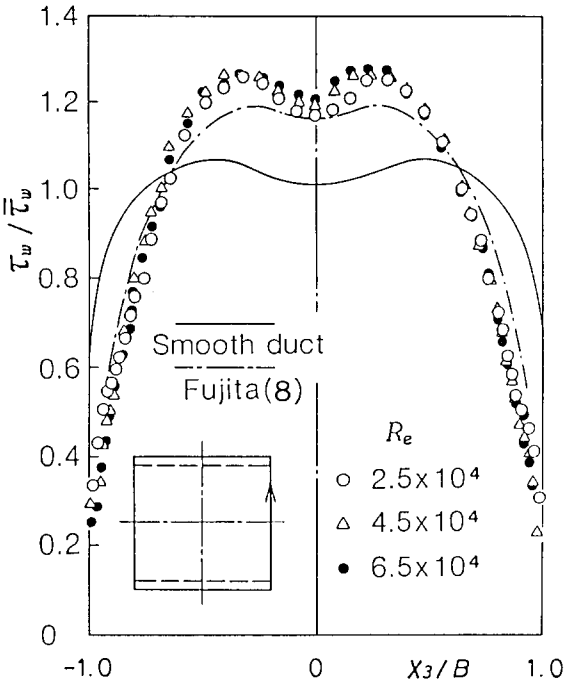

Figure 3 Wall shear stress distributions

and for the smooth wall, respectively:

$$\bar{\tau} = (\bar{\tau}_r + \tau_s)/2 \tag{4}$$

$\bar{\tau}_s$ can be calculated by using the results of the measurement with the Preston tube. The resulting value for the rough wall is equivalent to 43.1% of the total resistance of the duct. This means that one rough wall bears six times the resistance of one smooth wall. This is almost the same as the result in a rough duct[8] with two walls roughened by wires. It shows that the effects of a cross-sectional shape of roughness elements on the flow resistance may be slight when the heights of each roughness element are equal.

Mean velocities

In the rest of this paper, results of measurements are mainly shown by the contour maps. The values in each figure are the values nondimensionalized with U_S, the velocity at the center of the duct. The values of U_S differ from one another, depending on the axial velocity distribution of each duct. The ratios of U_S to the bulk mean velocity U were 1.22 for the smooth duct and 1.41 for the rough duct. As the contour maps obtained for U_1 in both the rough and smooth duct were extremely symmetrical with respect to the planes of geometrical symmetry of the duct cross section, results of velocities and stresses in half of the cross section are depicted. Broken lines, drawn in the upper and lower parts of each figure for the rough duct, show the height of roughness elements.

The contour map of the ratios of the axial mean velocity to the velocity at the center of the duct, or U_1/U_S, is shown in Figure 4. In the smooth duct, as is well known, the velocities at the corners are comparatively very large. In the rough duct, there is a zone of low velocity near a smooth wall, as observed in the smooth duct. But, near a rough wall, contours are almost straight and parallel to the wall. This suggests that the pattern of secondary flow differs from the one in the smooth duct.

Secondary flow vectors obtained from the measured results of U_2 and U_3 are shown in Figure 5. In the smooth duct, as shown in Figure 5(a), the well-known secondary flow is generated; namely, there are two secondary flow cells in each quadrant of a duct cross section. The secondary flow proceeds from the center of the duct toward the corner along the corner bisector and then outward in both directions. A duct-center-directed vector along the corner bisector is shown in the vicinity of the corner where the secondary flow changes its flow direction. The authors think that this may not be a real effect. It is possible that the frequently changing direction of the flow caused some error in measurement. In the rough duct, as clearly shown in Figures 5(b), (c), there is only one secondary flow cell in any given quadrant of a duct cross section. Secondary flow proceeds from the center of the duct toward the middle of a rough wall and then toward the middle of a smooth wall via a corner. In addition, the center of the secondary flow cell is off toward a smooth wall.

As stated in the previous section, secondary flows were measured at two cross sections of the rough duct; that is, one is 5 mm downstream of, and the other is atop of, the roughness element farthest downstream. The resulting vector diagrams are shown in Figure 5(b), (c). The main difference between the two diagrams is in the directions of vectors near the rough wall. This shows that the flow repeats separation at the roughness elements and reattachment downstream of the roughness elements. It follows that the flow is developed globally, but locally it changes in the neighborhood of roughness elements.

Fluctuation velocities and Reynolds stresses

The components of fluctuation velocity in each direction are shown in Figure 6 as contour maps of their ratios to U_S.

In the smooth duct, as shown in the left part of Figure 6(a), it is apparent that the contour lines of $\sqrt{\bar{u}_1^2}/U_S$ are more distorted than are those of axial mean velocity U_1. The curves show that the secondary flows transport lumps of low turbulence from the center to the corners. The present results of mean velocity and fluctuation velocity obtained by means of a hot-wire anemometer agreed well with the results of Melling and Whitelaw,[2] obtained by a laser Doppler anemometer. In the rough duct, as shown in the right half of Figure 6(a), a part of the profile is similar to that of a smooth duct in the bulges of contour lines near the X_2 axis, but the whole profile differs considerably from that of the smooth duct. The maximum value of $\sqrt{\bar{u}_1^2}/U_S$ in the rough duct is about 64% larger than that in the smooth duct, and the contour line corresponding to the maximum value lies near the center of the rough walls. A similar tendency in the distribution of contour lines near the rough wall is observed in a square duct with a rough wall.[7]

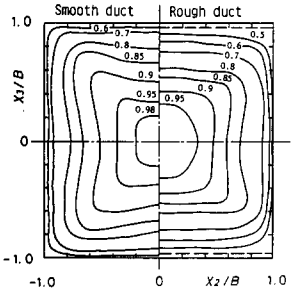

Figure 4 Axial mean velocity U_1/U_S

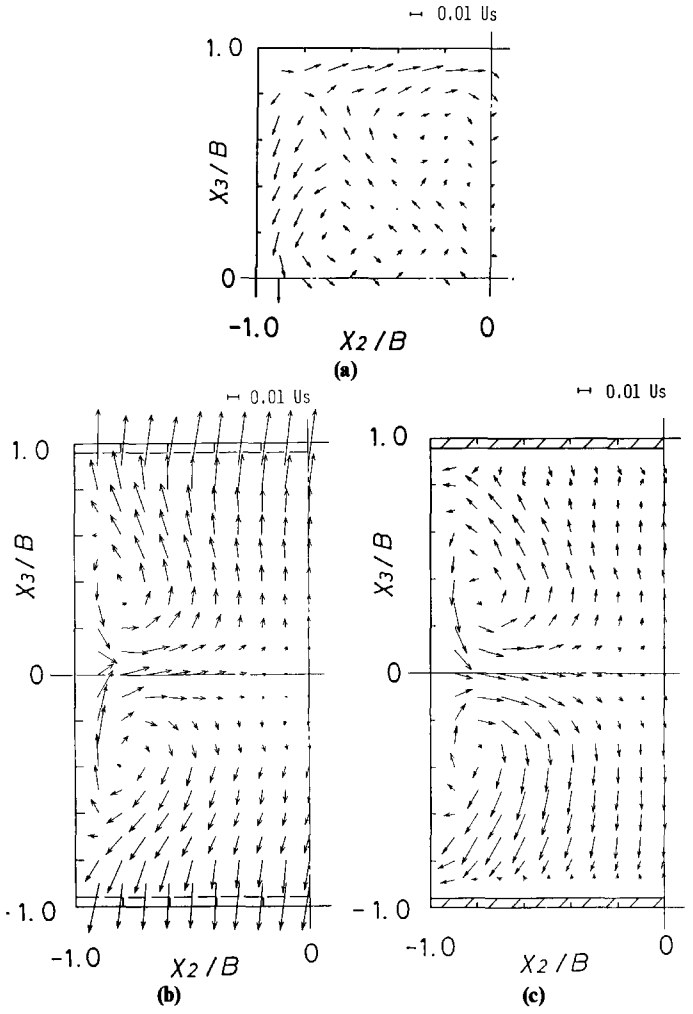

Figure 5 Secondary flow U_{SEC}: (a) smooth duct; (b) rough duct (downstream of roughness element); (c) rough duct (atop roughness element)

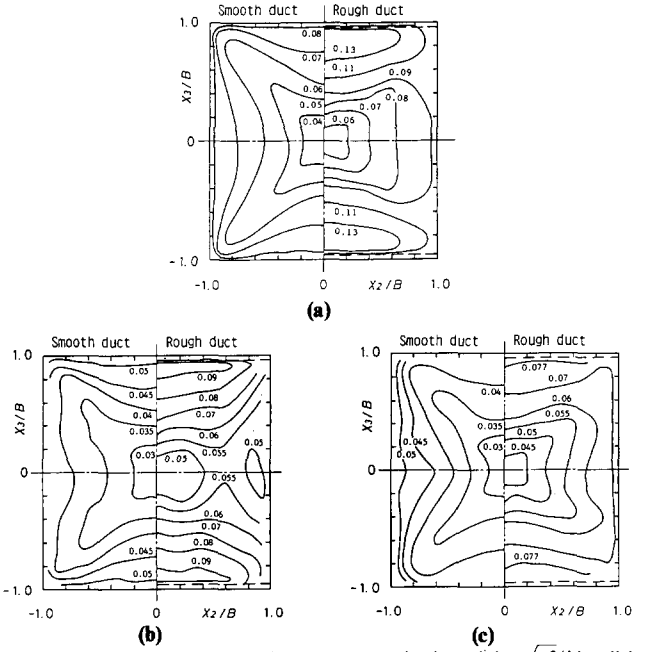

Figure 6 Components of fluctuation velocity: (a) $\sqrt{\bar{u}_1^2}/U_S$; (b) $\sqrt{\bar{u}_2^2}/U_S$; (c) $\sqrt{\bar{u}_3^2}/U_S$

Figures 6(b), (c) show contour maps of the components of fluctuation velocity in the directions perpendicular to a smooth wall and to a rough wall (in the directions of the X_2 and X_3 axes), respectively. In the smooth duct, the distribution profiles both of $\sqrt{\bar{u}_2^2}$ and $\sqrt{\bar{u}_3^2}$ are similar to that of $\sqrt{\bar{u}_1^2}$. But the magnitudes of the values of $\sqrt{\bar{u}_2^2}$ and $\sqrt{\bar{u}_3^2}$ are much smaller than that of $\sqrt{\bar{u}_1^2}$. In the rough duct, the largest values of $\sqrt{\bar{u}_2^2}$ and $\sqrt{\bar{u}_3^2}$ are shown to occur near the rough walls. Judging from that the largest value of $\sqrt{\bar{u}_2^2}$ is larger than that of $\sqrt{\bar{u}_3^2}$ near the rough wall, the effects of roughness elements would appear to be strongly in the direction normal to a smooth wall (in the X_2 direction). On the other hand, near the center of the smooth wall, $\sqrt{\bar{u}_2^2}$, a component of fluctuation perpendicular to the smooth wall, is constrained by the smooth wall while fluid lumps are transported by the secondary flow along the smooth wall and so have less value than $\sqrt{\bar{u}_3^2}$, a component of fluctuation parallel to the smooth wall.

The lateral components of turbulent shear stress, $\overline{u_1u_2}$ and $\overline{u_1u_3}$, are shown in Figures 7(a), (b), respectively. For the smooth duct, contour maps of $\overline{u_1u_2}$ and $\overline{u_1u_3}$ are symmetrical with respect to the diagonal of the duct. $\overline{u_1u_2}$ is equal to zero on the wall parallel to the X_2 axis and is, considering the symmetry of the duct, also equal to zero on the X_3 axis. Accordingly, the contour line for the value of zero forms a closed curve containing a part of the X_3 axis and a part of the wall. These results agree well with the results of Melling and Whitelaw.[2] As for the rough duct, the distribution profile of $\overline{u_1u_2}$ is quite different from that of the smooth duct, while there is not much difference in the magnitude of the values between $\overline{u_1u_2}$'s of the two ducts. On the other hand, there is little difference between the two ducts in the contour maps of $\overline{u_1u_3}$ except that the region bounded by the contour line for the value of zero in the rough duct is smaller than that in the smooth duct. The values of $\overline{u_1u_3}$ in the rough duct are much larger than those of the smooth duct.

Kinetic energy and vorticity

Some quantities and terms in a vorticity transport equation calculated from the measured results depicted above are shown in this section.

The contours of turbulent kinetic energy, $k=(\bar{u}_1^2+\bar{u}_2^2+\bar{u}_3^2)/2$, are shown in Figure 8. The profile resembles the $\sqrt{\bar{u}_1^2}$ profile, which is the largest of the three components of fluctuation velocity. To be specific, in the smooth duct contours bulge toward the corners along the corner bisectors, and the larger the values, the closer the corresponding curve lies to the wall. In the rough duct, the curve for the largest value of k lies closest

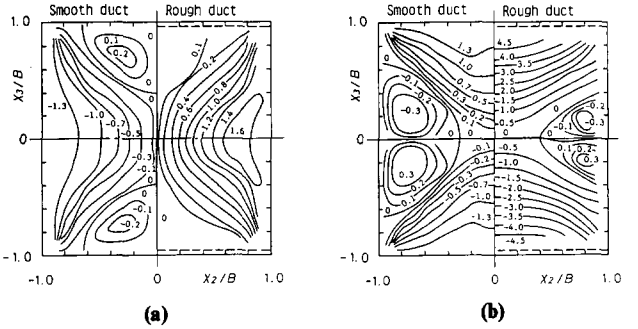

Figure 7 Reynolds shear stresses: (a) $\overline{u_1u_2}/U_S^2\times10^3$; (b) $\overline{u_1u_3}/U_S^2\times10^3$

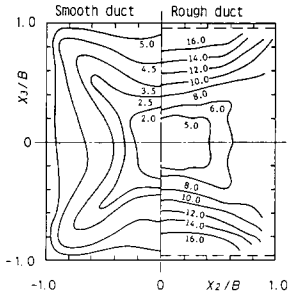

Figure 8 Turbulent kinetic energy $k=(\bar{u}_1^2+\bar{u}_2^2+\bar{u}_3^2)/(2/U_S^2)\times 10^3$

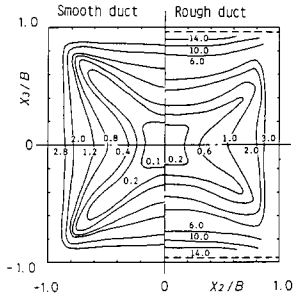

Figure 9 Turbulence production $-(\overline{u_i u_j}\,\partial U_i/\partial X_j)d_h/U_S^3\times 10^3$

to the rough walls, and the value here is three times as large as that in the smooth duct.

Figure 9 shows the contours of a turbulence production term in the turbulence energy equation.[14] The figure for the rough duct is similar to that of k, and the same is true for the smooth duct. As mentioned above, the contour lines of the components of fluctuation velocity are more distorted than those of the axial mean velocity. This is illustrated by comparing Figures 8 and 9: secondary flow proceeds from the center of the duct to the corners, and this gives rise to a steep gradient of axial mean velocity near the corners; then the steep velocity gradient may cause active production of turbulence.

Secondary flow of the second kind, shown in Figure 5, is generated and maintained by a nonhomogeneous and non-uniform turbulent stress field. This is understood by the examination of the streamwise vorticity transport equation for a steady incompressible flow expressed as

$$U_2\frac{\partial\Omega_1}{\partial X_2}+U_3\frac{\partial\Omega_1}{\partial X_3}=\frac{\partial^2}{\partial X_2\,\partial X_3}(\bar{u}_2^2-\bar{u}_3^2)+\left(\frac{\partial^2}{\partial X_3^2}-\frac{\partial^2}{\partial X_2^2}\right)\overline{u_2u_3}+\frac{\partial}{\partial X_1}\left(\frac{\partial\overline{u_1u_2}}{\partial X_3}-\frac{\partial\overline{u_1u_3}}{\partial X_2}\right)\qquad(5)$$

In Equation 5, terms related to the generation of the secondary flow of the second kind were retained on the right side. $\Omega_1=\partial U_3/\partial X_2-\partial U_2/\partial X_3$ denotes the component of mean vorticity in the X_1 direction, and the convection of Ω_1 by the secondary flow is represented by the terms on the left. Contour maps of Ω_1 and its convection are shown in Figures 10 and 11, respectively. Contours of Ω_1 for the smooth duct show the relation between Ω_1 and the location and the number of the generated secondary flow cells. In the rough duct, intensity of Ω_1 is high near the smooth walls and low near the center of the rough walls. The relation between the contours of Ω_1 and the secondary flow cells is not necessarily clear in the rough duct.

Terms on the right of Equation 5 represent the production of vorticity. Above all, $\bar{u}_2^2-\bar{u}_3^2$ is likely to make the most important contribution.[15] The contour maps of $(\bar{u}_2^2-\bar{u}_3^2)/U_S^2$ and its second partial derivative $[\partial^2(\bar{u}_2^2-\bar{u}_3^2)/\partial X_2\,\partial X_3]d_h^2/U_S^2$ are shown in Figures 12 and 13, respectively. As shown in the left part of Equation 12, contours are almost symmetrical with respect to the corner bisectors in the smooth duct. Consequently, the curve for $\bar{u}_2^2-\bar{u}_3^2=0$ almost coincides with the corner

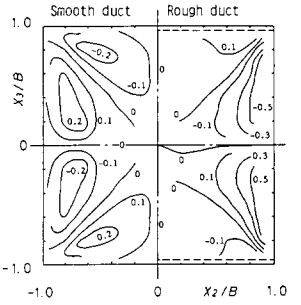

Figure 10 Streamwise vorticity $\Omega_1 d_h/U_S$

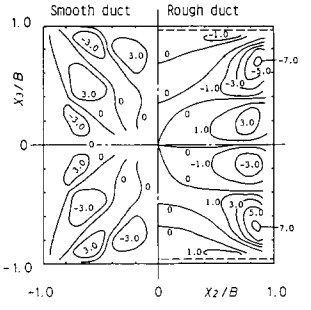

Figure 11 Convection of vorticity $(U_2\,\partial\Omega_1/\partial X_2+U_3\,\partial\Omega_1/\partial X_3)d_h^2/U_S^2\times 10^2$

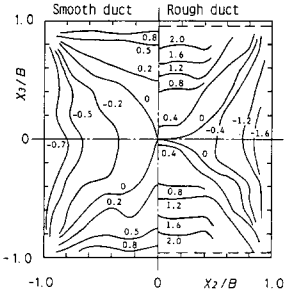

Figure 12 Difference of normal stresses $(\bar{u}_2^2-\bar{u}_3^2)/U_S^2\times 10^3$

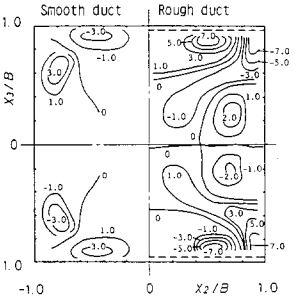

Figure 13 Production of vorticity $[\partial^2(\bar{u}_2^2-\bar{u}_3^2)/\partial X_2\,\partial X_3]d_h^2/U_S^2\times 10^2$

bisector. In the rough duct, the values of $\bar{u}_2^2-\bar{u}_3^2$ are considerably larger than those of the smooth duct. Furthermore, the curves for larger values near a rough wall are almost parallel to the rough wall. The curve for $\bar{u}_2^2-\bar{u}_3^2=0$ is off toward the smooth wall apart from the corner bisector. Figure 13, contour maps of a production term, shows there are regions of high intensity near the corners and near the walls in the smooth duct and near the corners and near the rough walls in the rough duct. Maximum intensity in the rough duct is nearly twice as large as that in the smooth duct.

If the term $\partial^2(\bar{u}_2^2-\bar{u}_3^2)/\partial X_2\,\partial X_3$ had the major effect on the generation of the secondary flow of the second kind, the term should have had nearly the same magnitude as the terms on the left of Equation 5, which show the convection of vorticity. As can be seen from Figures 11 and 13, in the smooth duct zones of vorticity production are balanced by vorticity convection away from these zones.[15] In the rough duct, as observed in the smooth duct, the balancing of the zones of vorticity production and convection was good. Although the importance of the $\overline{u_2u_3}$ contribution to the vorticity production was pointed out,[16] our discussion suggests that the $\overline{u_2u_3}$ contribution (which is expressed by the second term on the right side of Equation 5), may be smaller than the $\bar{u}_2^2-\bar{u}_3^2$ contribution, depending on the location in the duct cross section. We must discuss the matter on the basis of accurate measurements. Presently, however, there are experimental difficulties in measuring the $\overline{u_2u_3}$ stress component accurately.

Conclusions

Measurements were carried out on a fully developed turbulent flow along a square duct with roughened walls on two opposite sides. The experimental results as explained above lead to the following major conclusions.

(1) The coefficient of flow resistance in the duct with two rough walls is nearly three times larger than that of the smooth duct. And the two rough walls bear almost 86% of the total resistance of the duct. These results coincide with the results of the experiments where circular cross-sectioned roughness elements were used instead of square cross-sectioned ones.

(2) The magnitudes of the fluctuation velocities are large in the region near the center of the rough wall. The effect of roughness elements seems to appear strongly on the component in the direction normal to the smooth wall.

(3) The smooth square duct, as is well known, yields two secondary flow cells in any given quadrant of a cross section. The duct with rough walls on two opposite sides yields only one relatively large cell in each quadrant of the duct's cross section. The secondary flow proceeds from the center of the duct toward the middle of a rough wall and then toward the middle of the smooth wall via a corner.

(4) In the rough duct, the distribution of turbulent shear stress $\overline{u_1u_2}$ is quite different from that of the smooth duct. As for the distribution of $\overline{u_1u_3}$, there is little difference between the two ducts.

(5) In the rough square duct, zones of streamwise vorticity production are balanced by vorticity convection away from these zones, as has already been observed in the case of a smooth square duct.

References

1 Gessner, F. B. (Evaluator), Corner flow (secondary flow of the second kind). *Proceedings of the 1980-AFOSR-HTTM-Stanford Conference on Complex Turbulent Flows*, 1981, **1**, 182–212

2 Melling, A. and Whitelaw, J. H. Turbulent flow in a rectangular duct. *J. Fluid Mech.* 1976, **78**, 289–315

3 Gessner, F. B., Po, J. K., and Emery, A. F. Measurements of developing turbulent flow in a square duct. In *Turbulent Shear Flows I*, ed. F. Durst *et al.*, pp. 119–136. Springer, Berlin, 1979

4 Launder, B. E. and Ying, W. M. Prediction of flow and heat transfer in ducts of square cross-section. *Heat Fluid Flow* 1973, **3**(2), 115–121

5 Nakayama, A., Chow, W. L., and Sharma, D. Three-dimensional developing turbulent flow in a square duct. *Bull. Japan. Soc. Mech. Eng.* 1984, **27**(229), 1438–1445

6 Launder, B. E. and Ying, W. M. Secondary flows in ducts of square cross-section. *J. Fluid Mech.* 1972, **54**, 289–295

7 Humphrey, J. A. C. and Whitelaw, J. H. Turbulent flow in a duct with roughness. In *Turbulent Shear Flows 2*, ed. J. S. Bradbury *et al.*, pp. 174–188. Springer, Berlin, 1980

8 Fujita, H. Turbulent flows in square ducts consisting of smooth and rough planes. Research Report of the Faculty of Engineering, Mie University, 1978, **3**, 11–25

9 Fujita, H., Yokosawa, H., and Hirota, M. Measurements of turbulent flow through a square duct with a rough wall. Submitted to *Trans. ASME, J. Fluids Eng.*

10 Fujita, H., Yokosawa, H., and Hirota, M. Secondary flow to the second kind in rectangular ducts with one rough wall. *Experimental Thermal and Fluid Science* 1989, **2**, 72–80

11 Furuya, Y., Miyata, M., and Fujita, H. Turbulent boundary layer and flow resistance on plates roughened by wires. *Trans. ASME, J. Fluids Eng.* 1976, **98**, 635–644

12 Patel, V. C. Calibration of the Preston tube and limitations on its use in pressure gradients. *J. Fluid Mech.* 1965, **23**, 185–208

13 Hirota, M., Fujita, H., and Yokosawa, H. Influences of velocity gradient on hot wire anemometry with an X-wire probe. *J. Phys. E: Sci. Instr.* 1988, **21**, 1077–1084

14 See, for instance, Hinze, J. O., *Turbulence*, 2nd ed. McGraw-Hill, New York, 1975, p. 72

15 Brundrett, E. and Baines, W. D. The production and diffusion of vorticity in duct flow. *J. Fluid Mech.* 1964, **19**, 375–394

16 Perkins, H. J. The formation of streamwise vorticity in turbulent flow. *J. Fluid Mech.* 1970, **44**, 721–740